REFLECTIVITY CHARACTERIZATION AND IDENTIFICATION OF PRIMARY REFLECTION PATH IN ANECHOIC CHAMBER ANALYSIS

Aloysius Aragon Lubiano
Raytheon, 2000 East Imperial Highway
RE/R01/A566, El Segundo, CA 90245

Christopher R. Brito
Lockheed Martin
1111 Lockheed Martin Way, Sunnyvale, CA 94089

Newlyn Hui
L3 Communications, Randtron Antenna Systems
130 Constitution Dr., Menlo Park, CA 94025

Dean Arakaki
California Polytechnic State University, Electrical Engineering Department
1 Grand Avenue, San Luis Obispo, CA 93401

ABSTRACT

This paper presents an analysis of the reflectivity performance of the anechoic chamber. Measurements indicating the performance of the chamber-installed foam absorbers (described in a companion paper) are used to complete this analysis. This is followed by a comparison of the analysis results to chamber measurements taken in accordance with the free-space VSWR procedure [1]. Agreement between the analysis results and worst-case VSWR test measurements is within 1dB for a majority of reflection angles. In addition to chamber performance predictions, this paper describes a method of identifying primary reflection paths through interferometer calculations that compare all single bounce reflection path lengths to the direct path length. The angular spacing between interferometer nulls is used to identify the primary reflection direction. This information can be used to improve the overall chamber reflectivity by identifying areas of significant reflections and enhancing absorber treatments in these areas.

Keywords: Anechoic Chamber, Chamber Reflectivity, Quiet Zone, Ray Tracing, Interferometer Analysis

1. Introduction

Anechoic chambers enable the characterization of antennas in an open space environment simulated by absorber foam installed on the chamber walls. In the test region, the so-called ‘quiet zone,’ both the magnitude and phase of the radiation emitted by the transmit antenna is uniform to within a specified range corresponding to an overall chamber reflectivity level.

The overall reflectivity of an anechoic chamber can be predicted by a ray-tracing analysis using reflectivity data from the absorber foam over various incidence angles and signal frequencies. The foam reflectivity characterization described in a companion paper is used to predict the overall chamber performance and compared with values calculated from measurements via the free-space VSWR test [2]. Over the operating range of frequencies (2.6GHz to 18GHz), the ray-tracing prediction and actual measurements differed by less than 1 dB for a majority of the measured scan data.

The free-space VSWR test described in [2] involves the measurement of electric field magnitude and phase within the quiet zone (test region). The electric field is measured as a function of position both along and transverse to the length axis of the chamber. The probe antenna is also rotated following each scan to determine worst-case reflectivity levels with respect to direction. This allows identification of the direction from which the most significant reflections occur.

While the free-space VSWR measurement technique converts raw measurement data into useful overall reflectivity values for the chamber, it does not identify the primary reflection path from among the multiple reflection paths that comprise the overall reflection level. This paper describes a technique that uses the ripple in the received field pattern as a function of scan coordinate to determine the dominant reflection path. The overall chamber performance can then be enhanced by adjusting absorber placement and/or coverage in the region(s) identified by this analysis technique.

2. Approach

The overall reflectivity performance of the chamber is analyzed using a ray-tracing technique that maps the location of images that produce the reflected signals (see Fig. 1 in the appendix).

Four rays are considered for each side wall: paths A through D. The one-bounce reflection paths include rays A and C, where ray A reflects from the back wall, while ray C reflects once in the specular region on the side wall. The two-bounce reflection paths include rays B and D as shown in Fig. 1. It is assumed that reflection paths involving more than two reflections will have negligible intensity due to attenuation by the foam. The anechoic chamber is partially lined with wedge foam; however, all four single-reflection paths involve regions populated with pyramid-shaped absorbers only.

The values of the incidence angles shown in Fig. 1 are summarized along with pyramid-shaped absorber reflectivity values at the specified angles in Table 1 below.

Table 1 Incident Angle and Absorber Reflectivity Summary for Reflection Paths B through D

Incident Angle	**θ_1= 36.3°** Ray B	**θ_2=56.3°** Ray C	**θ_3= 68.2°** Ray D	**θ_4=21.8°** Ray D	**θ_5=36.3°** Ray B
Reflectivity	**-42 dB**	**-40 dB**	**-30 dB**	**-42 dB**	**-42 dB**

Note that pyramid foam reflectivity at incidence angles less than 40° exhibit reflectivity levels consistent with normal incidence values. The reflection levels reaching the quiet zone are summarized in Table 2.

Combining reflectivity values with spreading (path) loss due to propagation distance, the worst-case total reflectivity has been calculated to be -40.3dB or -46.9dB using the direct sum (all reflections in phase) and root- sum-square (random phases) techniques, respectively.

Table 2 Quiet Zone Reflectivity Analysis Summary

Ray	# of Rays	# of Bounce	Aut D (dB)	1st Reflect (dB)	2nd Reflect (dB)	Path Loss (dB)	Ray Mag (dBm)
A	1	1	0	-45	--	-4.44	-49.44
B	4	2	-17.3	-42	-42	-4.44	-105.77
C	4	1	-14.7	-40	--	-1.6	-56.47
D	4	2	-6.1	-30	-42	-5.08	-83.18

3. Test Results

Both longitudinal and transverse (parallel and normal to chamber length axis) scans of the total electric field amplitude reaching the quiet zone have been taken as a function of rotational (aspect) angle at 10° increments. A summary for the transverse scan is presented in Fig 2 (appendix).

The chart in Fig. 2 indicates a worst-case reflectivity level of -36.29dB at an aspect angle of 40°. Using the relation between antenna pattern level (PL), chamber reflectivity (R), and pattern ripple (r) [1],

$$r = \frac{PL + R}{PL - R} \qquad (1)$$

pattern levels to -15dB below the mainbeam peak can be measured with 1dB of ripple on the measurement. At the -20dB level, the ripple is approximately 1.7dB.

Once the maximum reflectivity direction has been determined, the dominant reflection path is identified from among the multiple paths followed by reflected signals that comprise the overall reflection level. The transverse scan for the 40° aspect angle is shown in Fig. 3 below and is analyzed to determine the primary reflection path interfering with the direct path signal.

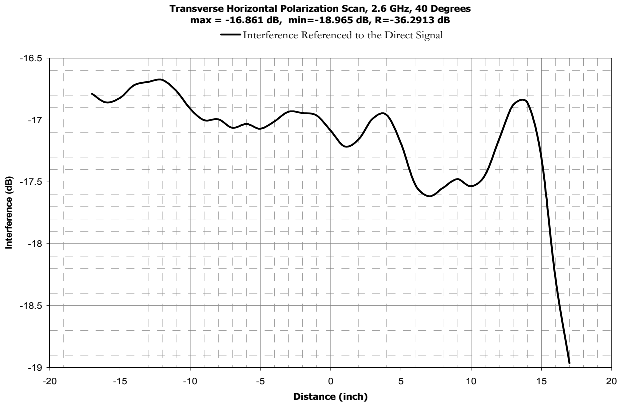

Fig. 3 Transverse Horizontal Polarization Scan

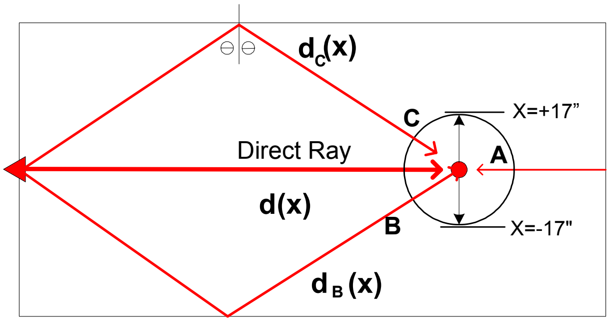

Fig. 4 Direct and All Single-Reflection Paths to the Quiet Zone

An interferometer analysis is carried out to identify the primary reflection path interfering with the direct signal from the transmit to the receive horn. Since reflections from the absorber foam is out of phase with respect to the direct signal (due to a higher foam permittivity compared to free-space), nulls in the scan pattern occur when the path difference between the direct and reflected signal is an integral number of wavelengths. Coordinates along the scan path where signal cancellation occurs are calculated for all single-bounce reflection paths and compared to the actual scan pattern (see Fig. 4).

The distances along all four paths defined in Fig. 4 as a function of transverse displacement *x* are given by the relations below.

$$d(x) = \sqrt{(180'')^2 + x^2} \tag{2}$$

$$d_A(x) = 240'' + \sqrt{(60'')^2 + x^2} \tag{3}$$

$$d_B(x) = \sqrt{(180'')^2 + (103'' + |x + 17''|)^2} \tag{4}$$

$$d_C(x) = \sqrt{(180'')^2 + (103'' + |x - 17''|)^2} \tag{5}$$

It was determined that path C is the dominant reflection path to the quiet zone. This reflected signal interferes with the direct signal to produce a ripple pattern with nulls occurring at scan coordinates where the difference between the direct and ray C paths differ by a multiple of a wavelength.

4. Conclusions

This paper presents an overall reflectivity analysis of Cal Poly's recently constructed Anechoic Chamber. Both longitudinal and transverse (to the chamber length axis) scans have been measured in accordance with the free-space VSWR test outlined in [2]. It was determined that the worst-case reflectivity level is approximately -40dB which allows pattern measurements -15dB (-20dB) below the mainbeam peak with a maximum pattern ripple of 1dB (1.7dB).

An interferometer analysis (direct and reflected signal interference) is performed to identify the dominant reflection path. Scan coordinates at which interferometer nulls will occur are calculated for all single-bounce reflection paths. The primary reflection path is identified by selecting the scan response that best correlates the predicted with the actual nulls in the scan patterns. It was determined that the single-bounce reflection from the specular region in the sidewall contributed the worst-case reflection at the 40° aspect angle.

5. References

[1] Hemming, L.H., *Electromagnetic Anechoic Chambers*, 2002, Piscataway, NJ: IEEE Press.
[2] Appel-Hansen, J., "Reflectivity Level of Radio Anechoic Chambers, *IEEE Trans. Antennas Propagat.*, vol. AP-21, no. 4, July 1973.
[3] *IEEE Std 1128-1998*, IEEE Recommended Practice for Radio-Frequency (RF) Absorber Evaluation in the Range of 30 MHz to 5 GHz. 1998, New York: IEEE Press.

6. Acknowledgements

The authors would like to thank Deskin Research, Raytheon, and Lockheed Martin for material donations and the employees of Lockheed Martin and JPL for technical support during the construction and testing of the Cal Poly Anechoic Chamber. We would also like to thank Cal Poly's Center for Teaching and Learning for support through the University Summer Services and Fall Faculty Development Grant Programs and Cal Poly's Electrical Engineering Department for financial support of the chamber project through the purchase of absorber foam.

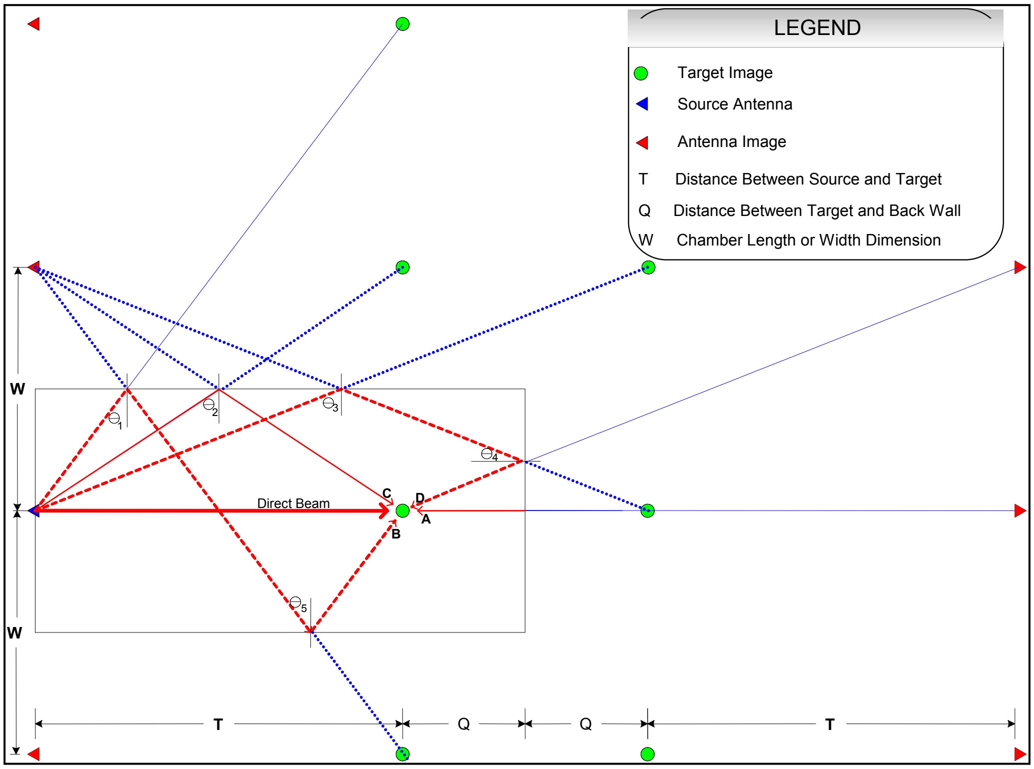

Fig. 1 Ray-Tracing Method with Image Positions

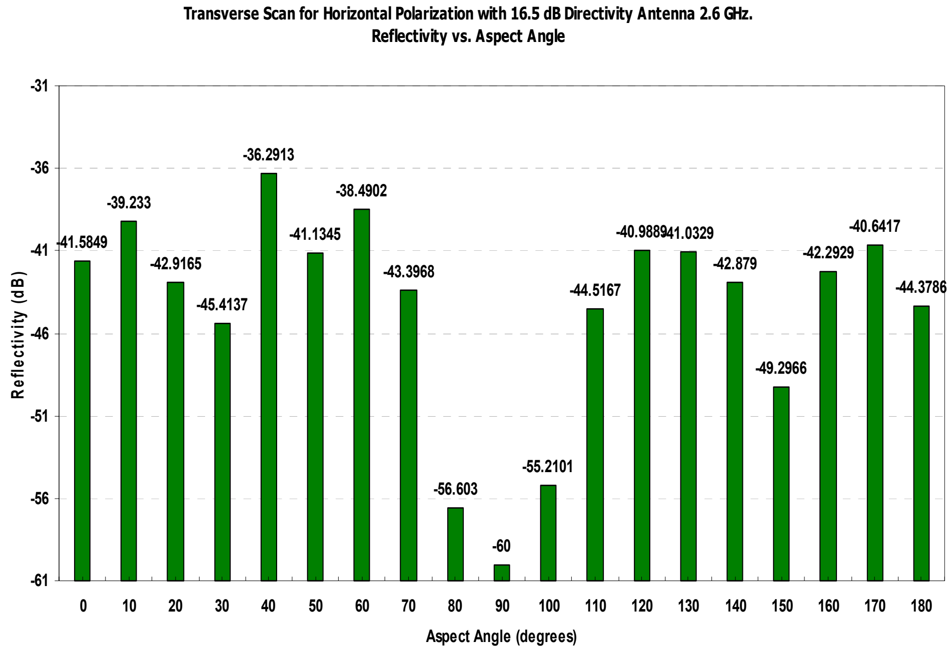

Fig. 2 Reflectivity Levels *vs*. Aspect Angle, Transverse Scan